



Contents lists available at ScienceDirect

## Earth and Planetary Science Letters

journal homepage: [www.elsevier.com/locate/epsl](http://www.elsevier.com/locate/epsl)

## A 56 million year rhythm in North American sedimentation during the Phanerozoic

Stephen R. Meyers\*, Shanan E. Peters

Department of Geoscience, 1215 W. Dayton Street, University of Wisconsin-Madison, Madison, WI 53706, USA

## ARTICLE INFO

## Article history:

Received 20 August 2010  
 Received in revised form 14 December 2010  
 Accepted 20 December 2010  
 Available online xxxx

Edited by P. DeMenocal

## Keywords:

macrostratigraphy  
 cyclostratigraphy  
 sedimentation  
 spectral analysis  
 biologic diversity

## ABSTRACT

Long-term (>10 Myr) fluctuations in climate, sea-level and sedimentation have been documented in the stratigraphic record, but the lack of well-constrained data series has made it difficult to rigorously evaluate cyclic (periodic or quasi-periodic) changes at this scale. Here we utilize a new compilation of the coverage area of sedimentary rocks in North America to investigate the dominant modes (“orders”) of stratigraphic variability, and to evaluate potential long-period cyclic changes in sedimentation on the continent during the Phanerozoic. Our analysis resolves two principal temporal modes of variability: (1) a strongly sinusoidal mode with a periodicity of 56 Myr  $\pm$  3 Myr, and (2) a longer-term Phanerozoic mode (the “M-curve”, linked to the Wilson cycle), which is indistinguishable from a stochastic autoregressive process. The newly identified 56 Myr cycle in sedimentation delineates most of the cratonic sequences that have previously been identified qualitatively in North America, but here we propose a quantitative redefinition that includes nine distinct units and two mega-sequences. The timing of the 56 Myr beat in sedimentation is consistent with an orogenic oscillator source or an oscillatory dynamic in mantle convection, and its tempo is statistically similar to a known rhythm in number of marine animal genera in the global fossil record. Thus, the identification of a significant periodic signal in the sedimentary record of North America provides new evidence for an important tectonic- and/or mantle-scale cyclic process that links both large-scale biological evolution and physical environmental change.

© 2010 Elsevier B.V. All rights reserved.

## 1. Introduction

Rhythmic changes in climate, sea-level and sedimentation are a prominent feature of the Neogene, fundamentally linked to interactions between orbital-insolation and cryosphere dynamics (Clark et al., 1999; Hays et al., 1976; Lisiecki, 2010; Zachos et al., 2001). Although longer-term (>10 Myr) fluctuations in climate, sea-level and sedimentation are known to occur (Haq et al., 1987; Kominz, 1995; Miller et al., 2005; Vail et al., 1977), the lack of well-constrained, high-resolution data on the character and extent of sedimentary rocks has prevented rigorous quantitative analysis of their cyclic temporal variability. In this study, we utilize the total coverage area of sedimentary strata, derived by macrostratigraphic analysis of the rock record of North America (Peters, 2006), to (1) extract the dominant modes (“orders”) of stratigraphic variability, and (2) evaluate potential long-period cyclic changes in sedimentation during the Phanerozoic. This continent-scale record reflects both the production and preservation of sediments, factors that are governed by large-scale crustal deformation, mantle-controlled dynamic topography, global eustatic sea-level, and climate (Miall, 1997). Our novel approach to this research problem integrates emerging macrostratigraphic and cyclostratigraphic methods to

provide a robust quantitative foundation for evaluation of the stratigraphic record.

## 2. Material and methods

A comprehensive macrostratigraphic database (Peters and Heim, 2010) consisting of 18,815 sedimentary rock units from 814 geographic locations in North America (Fig. 1) is used to estimate total sediment coverage area ( $A_{sed}$ ), primarily based upon published correlation charts for the United States (Childs, 1985; Salvador, 1985) and Canada (Douglas, 1970). The database (accessible at <http://macrostrat.geology.wisc.edu>) includes most known rock units from both the surface and subsurface, and utilizes stage boundary ages from the most recent International Stratigraphic Chart (International Commission on Stratigraphy; <http://www.stratigraphy.org/upload/ISChart2009.pdf>). To determine the areal extents of sedimentary rock units, a Dirichlet tessellation (Fig. 1b) around each of the 814 stratigraphic column control points (Fig. 1a) is calculated using the Delaunay triangulation function in the ‘deldir’ package for R (R development core team, 2006). The spacing of columns and the resultant areas generally reflect the complexity of the geological record of that region, with continental margins having, on average, a closer packing of columns than the sediment-covered continental interior. In the absence of data to the contrary, we presume that the areal extent of rock units that occur in one column but not in an adjacent column extends half-way between the two.

\* Corresponding author. Tel.: +1 608 890 2574; fax: +1 608 262 0693.  
 E-mail address: [smeyers@geology.wisc.edu](mailto:smeyers@geology.wisc.edu) (S.R. Meyers).

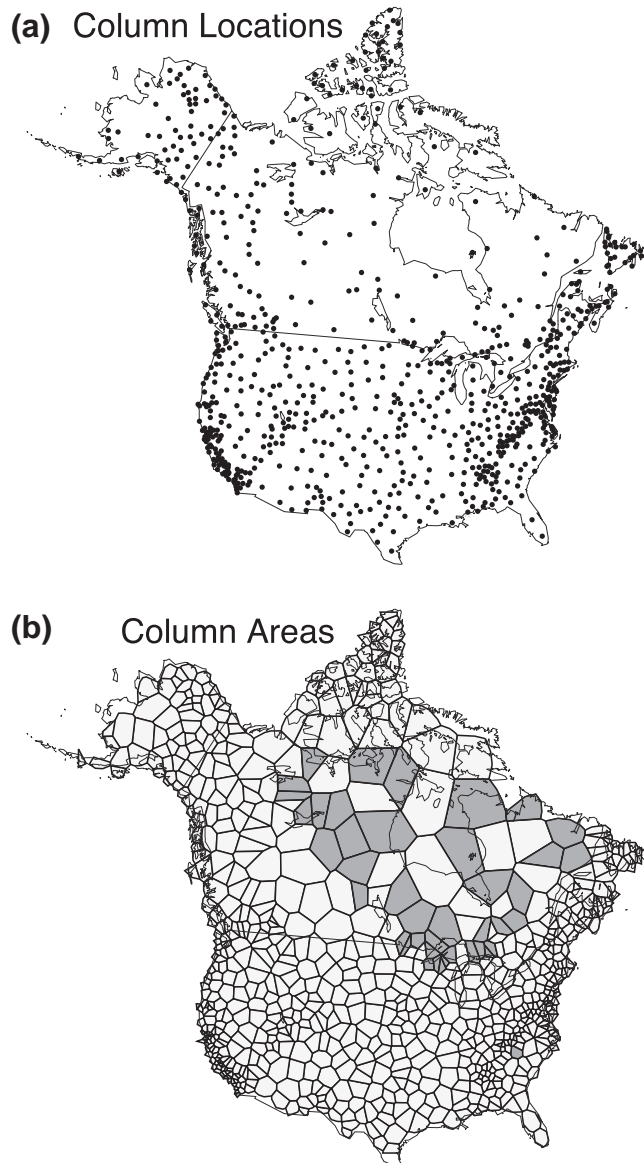


**Fig. 1.** Geographic distribution of sampling regions for macrostratigraphic analysis. a, Location of all 814 geologic column control points. b, Interpolated areas represented by each column. Dark polygons have no pre-Pleistocene sedimentary cover.

$A_{\text{sed}}$  is estimated for each Phanerozoic time interval by summing the area of all polygons that preserve at least one sedimentary rock unit of that age. Our analysis of  $A_{\text{sed}}$ , which includes all terrestrial and marine sedimentary rocks that are present at both the Earth's surface and in the subsurface, is complimented by a preliminary assessment of the coverage area of marine strata ( $A_{\text{mar}}$ ). We only tentatively interpret the  $A_{\text{mar}}$  data here, as its determination is complicated by uncertainties associated with the partitioning of marine and terrestrial deposits in the macrostratigraphy database (a subject of ongoing work). The  $A_{\text{sed}}$  and  $A_{\text{mar}}$  data series have an average sampling resolution of 6.6 Myr ( $\pm 3.5$  Myr,  $1\sigma$ ), and approximately 85% of the data are characterized by a sample spacing of  $\leq 10$  Myr. Neither  $A_{\text{sed}}$  nor  $A_{\text{mar}}$  indicates a significant correlation between area and temporal bin size ( $r^2$  of 0.004 and 0.021, respectively), indicating that this is not a substantial source of bias. Both data sets are linearly interpolated to a resolution of 1 Myr prior to time series analysis, but to account for limitations of the original sampling resolution, all analyses are conservatively restricted to frequencies  $< 1/20$  Myr $^{-1}$ .

To evaluate the dominant modes of variability, and to test for cyclic changes in  $A_{\text{sed}}$  and  $A_{\text{mar}}$ , we apply three complimentary statistical

approaches: multi-taper method (MTM) spectral analysis (Thomson, 1982), evolutive harmonic analysis (EHA; Meyers et al., 2001), and singular spectrum analysis (SSA; Ghil et al., 2002). MTM spectral analysis permits the identification and deconvolution of periodic, quasi-periodic and broadband stochastic noise variance (Mann and Lees, 1996; Meyers et al., 2008; Thomson, 1982). We evaluate the  $A_{\text{sed}}$  and  $A_{\text{mar}}$  power spectra against a stochastic red noise process, which is estimated by fitting an autoregressive [AR(1)] model to a log-transformed median smoothed version of the MTM power spectra (Mann and Lees, 1996). The red noise hypothesis test is supplemented with an independent MTM harmonic F-test for the identification of phase-coherent sinusoids (periodic components; Thomson, 1982). Frequency bands that exceed both the 99% red noise confidence level and 99% harmonic F-test confidence level provide strong confirmation of cyclic variability. To further investigate the persistence and temporal evolution of hypothesized cycles, time-frequency analysis (EHA) is applied to the  $A_{\text{sed}}$  and  $A_{\text{mar}}$  data series.

Singular spectrum analysis (SSA) is utilized to extract the dominant modes of variability within the “delay-coordinate” phase space for  $A_{\text{sed}}$  and  $A_{\text{mar}}$  (Ghil et al., 2002). This technique enables the identification of both oscillatory and non-oscillatory signals, and provides an objective approach by which to define multiple “orders” of stratigraphic variability. Of note, in contrast to Fourier and wavelet-based methods, SSA does not force decomposition of the data series to a prescribed basis set (e.g., sinusoids).

Our investigation of  $A_{\text{sed}}$  is paired with an assessment of macrostratigraphic truncation, initiation and turnover rates (Peters, 2006). These parameters are stratigraphic analogs of the commonly used paleobiologic metrics (Foote, 2000), where the fundamental unit is a “hiatus-bound” sedimentary package (see Peters, 2006). As in previous studies (Hannisdal and Peters, 2010), chronostratigraphic gaps are defined as time intervals that exceed the level of resolution employed by the compilation, which is approximately 1 to 3 Myr. Four classes of gap-bound packages can be recognized for any given stratigraphic interval: those confined to the interval (FL), those that only cross the bottom boundary (bL), those that only cross the top boundary (Ft) and those that cross both boundaries (bt) (Fig. 2; Hannisdal and Peters, 2010; Peters, 2006). Estimated macrostratigraphic rates assume a Poisson process for the probability of persistence across contiguous stratigraphic intervals, and thus are determined as (Foote, 2000; Peters, 2006):

$$\begin{aligned} \text{Truncation Rate} &= -\ln(X_{\text{bt}} / (X_{\text{bt}} + X_{\text{bL}})) / \Delta t \\ \text{Initiation Rate} &= -\ln(X_{\text{bt}} / (X_{\text{bt}} + X_{\text{Ft}})) / \Delta t \\ \text{Turnover Rate} &= \text{Initiation Rate} - \text{Truncation Rate} \end{aligned}$$

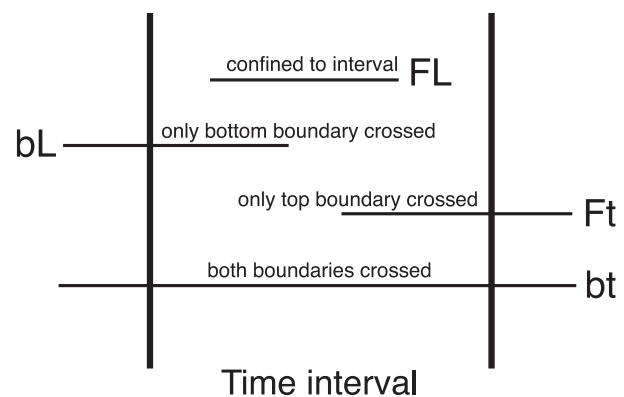


**Fig. 2.** Four classes of gap-bound packages can be recognized for any given stratigraphic interval: those confined to the interval (FL), those that only cross the bottom boundary (bL), those that only cross the top boundary (Ft) and those that cross both boundaries (bt). Figure adapted from Peters (2006).

where  $\Delta t$  = time interval,  $X_{bt}$  = number of gap bound packages that cross both the lower and upper time interval boundaries,  $X_{bl}$  = number of gap bound packages that only cross the lower time interval boundary,  $X_{Ft}$  = number of gap bound packages that only cross the upper time interval boundary.

### 3. Results

MTM power spectral analysis indicates that most of the variance observed in the  $A_{sed}$  data series can be explained by a stochastic autoregressive model (at the 99% confidence level), with the exception of a region of power centered on a frequency of  $1/56$  Myr (Fig. 3c). MTM harmonic F-test results confirm the presence of a highly significant (>99.9% confidence level) phase-coherent sinusoid in  $A_{sed}$ , exhibiting a periodicity of 56 Myr (Fig. 3b). The variance attributable to this frequency component (gray area in Fig. 3c), once deconvolved from the  $A_{sed}$  power spectrum (Thomson, 1982), yields an estimate of the residual spectrum that is consistent with the autoregressive red noise model. The 56 Myr cycle accounts for 14% of the observed variance in the  $A_{sed}$  power spectrum ( $<1/20$  Myr<sup>-1</sup>), and uncertainty in its true periodicity is estimated to be 56 Myr  $\pm$  3 Myr ( $\pm 0.5 f_{ray}$ ;  $f_{ray}$  = Rayleigh resolution). EHA of the  $A_{sed}$  record reveals the temporal evolution of this 56 Myr beat (Fig. 3d), which is persistent throughout most of the Phanerozoic, with the notable exception of a gap at approximately 325 Ma.

SSA extracts two dominant modes of variability in the  $A_{sed}$  data series: (1) a sinusoidal mode with variance concentrated at a frequency of  $\sim 1/56$  Myr<sup>-1</sup> (Fig. 3a and Fig. 4b), and (2) a longer-term Phanerozoic mode (Fig. 4a). Together, these modes of variability account for 95% of the variance in  $A_{sed}$  (Fig. 4c), with the 56 Myr oscillation (Fig. 4b) representing 19% of the total variance. Thus, the SSA results for the  $A_{sed}$  data series afford strong independent confirmation of the MTM and EHA results, and also corroborate a diminishment of the 56 Myr cyclic signal at  $\sim 325$  Ma (Fig. 3). The SSA results further highlight a relatively diminished 56 Myr cyclic variability in  $A_{sed}$  during the Cenozoic.

Finally, comparison of the extracted 56 Myr rhythm (Fig. 4b) with the independently estimated macrostratigraphic rates (Fig. 4d) illustrates that most of the observed oscillations are associated with an increase in macrostratigraphic package initiation and/or truncation rate (asterisks in Fig. 4d). Based on these results, we conclude that the 56 Myr  $A_{sed}$  cycle is a consequence of changes in both package initiation and truncation rate, but the relative importance of these two distinct phenomena is variable. The highest magnitude package turnover rates (initiation-truncation; Fig. 4d) are observed at the Cretaceous–Paleogene boundary, the Permian–Triassic boundary, and the middle Ordovician ( $\sim 465$  Ma), all of which are preceded by pronounced negative turnover rates that reflect a reduction in the area of sedimentation. In total, these truncation, initiation, and turnover rate responses are diagnostic of geographic expansion of erosion/non-deposition (sea-level fall and “sequence boundary”

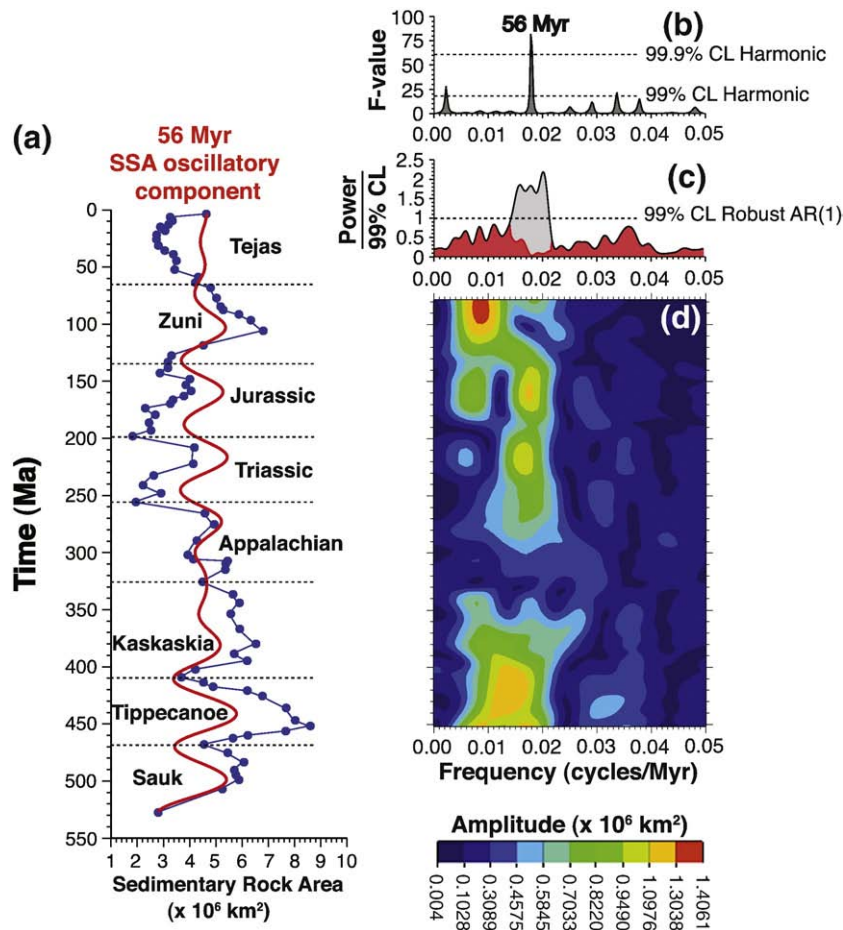


**Fig. 3.** Cyclic variation in North American sedimentation. a, Area of preserved sedimentary strata ( $A_{sed}$ ) in North America during the Phanerozoic (blue), with North American sequences (Peters, 2008; Sloss, 1963) and a 56 Myr oscillatory component extracted using SSA (red). b, MTM harmonic F-test spectrum for  $A_{sed}$ , calculated using three  $2\pi$  prolate tapers (Thomson, 1982). Dashed lines indicate the 99% and 99.9% confidence levels for F-values. c, MTM power spectrum for  $A_{sed}$ , calculated using adaptive weighting and three  $2\pi$  prolate tapers (Thomson, 1982). Total power has been divided by the 99% confidence level for a robust AR(1) red noise model (Mann and Lees, 1996). Grey area indicates power attributable to the 56 Myr phase-coherent sinusoid identified in part b, following spectral reshaping (Thomson, 1982). d, EHA of  $A_{sed}$ , using three  $2\pi$  prolate tapers and a 150 Myr moving window. A linear trend has been removed from each 150 Myr data window prior to harmonic analysis.

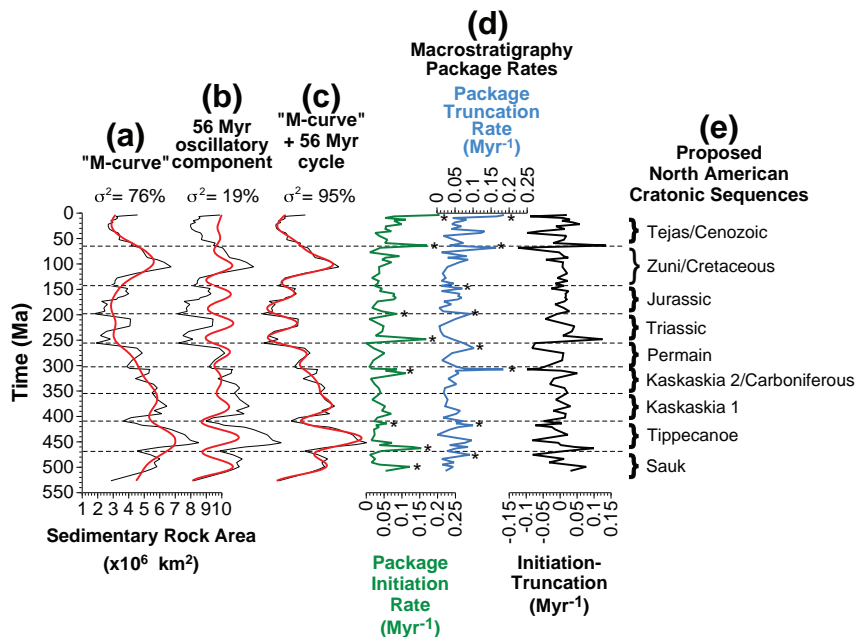


**Fig. 4.** Singular spectrum analysis (SSA) results for the  $A_{\text{sed}}$  data series, as compared to macrostratigraphy package rates. The  $A_{\text{sed}}$  data series is shown as a thin black line, and the SSA reconstructions are shown in red. SSA utilizes an embedding dimension of 80 with the Vautard and Ghil covariance estimator (Ghil et al., 2002), and extracts four dominant reconstructed components (RCs). a, RC 1 and RC 2 (combined), which comprise the long term Phanerozoic “M-curve”. b, RC 3 and RC 4 (combined) constitute an oscillatory pair with variance concentrated at a frequency of  $\sim 1/56 \text{ Myr}^{-1}$ . c, Total SSA reconstruction, which incorporates RC 1, RC 2, RC 3 and RC 4, and accounts for 95% of the variance in  $A_{\text{sed}}$ . d, Package initiation rate (green), package truncation rate (blue), and initiation rate–truncation rate (black), determined by macrostratigraphic analysis. Initiation and truncation rates are calculated according to the estimated per-package per million-year rate adapted from Foote (2000). e, Designation of major North American cratonic sequences based on macro-cyclostratigraphic analysis. (For interpretation of the references to color in this figure legend, the reader is referred to the web version of this article.)

development) followed by sea-level rise and the restoration of sediment accumulation and preservation. This is in contrast to the Triassic/Jurassic boundary, for example, where truncation and initiation rate responses are characterized by a degree of covariation, indicating changing loci of deposition on the continent, but also a general reduction in the area of sedimentation (Fig. 4).

The Permian–Triassic and middle Ordovician turnover maxima noted above approximately coincide with minima in the 56 Myr  $A_{\text{sed}}$  cycle (Fig. 4). The lack of a strong 56 Myr  $A_{\text{sed}}$  minimum associated with the Cretaceous–Paleogene boundary is potentially due to the increased influence of terrestrial sediment during the Cenozoic (up to 72% of the area), in contrast to pre-Cenozoic sediments, which are dominated by marine strata (Peters, 2006; averaging 92% of the area). This hypothesis is supported by a separate analysis of the area of marine strata ( $A_{\text{mar}}$ ), documented below, which indicates a  $\sim 55 \text{ Myr}$   $A_{\text{mar}}$  minimum associated with the Cretaceous/Paleogene boundary (Figs. 5 and 6).

Preliminary analysis of the coverage area of marine strata ( $A_{\text{mar}}$ ), yields similar results, although generally of lower statistical significance (Fig. 5). The noisier nature of  $A_{\text{mar}}$  (relative to  $A_{\text{sed}}$ ) may correctly characterize the nature of marine sedimentation on North America, or alternatively, it could be due to inaccuracies in the partitioning of marine and terrestrial deposits in the current version of the macrostratigraphic database. Given the present status of the  $A_{\text{mar}}$  data series, we tentatively identify a  $55 \text{ Myr} \pm 3 \text{ Myr}$  ( $\pm 0.5 f_{\text{ray}}$ ) cycle that accounts for 8% of the variance observed in the  $A_{\text{mar}}$  power spectrum ( $< 1/20 \text{ Myr}^{-1}$ ), a 55 Myr oscillatory signal extracted by SSA, constituting 13% of the  $A_{\text{mar}}$  variance (Figs. 5a and 6b), and a long-term Phanerozoic mode accounting for 83% of the  $A_{\text{mar}}$  variance (Fig. 6a). A notable distinction between  $A_{\text{mar}}$  and  $A_{\text{sed}}$  is the indication of a strong  $\sim 55 \text{ Myr}$  SSA oscillation in marine sedimentation during the Cenozoic, and distortion (elongation) of the SSA oscillation during the “Zuni” cycle (compare Figs. 4b and 6b). Both  $A_{\text{mar}}$  and  $A_{\text{sed}}$  reveal a diminishment of the oscillatory signal centered on  $\sim 325 \text{ Ma}$ . Minima in the  $\sim 55 \text{ Myr}$   $A_{\text{mar}}$  rhythm approximately coincide with maxima in

package turnover rates observed at the Cretaceous–Paleogene boundary, the Permian–Triassic boundary, and in the middle Ordovician (Fig. 6).

#### 4. Discussion

Building upon the previous work of Sloss (1963) and Peters (2008), our macro-cyclostratigraphic analysis of North America motivates a redefinition of the North American cratonic sequences. We propose nine individual  $\sim 56 \text{ Myr}$ -long cratonic sequences (Figs. 4e and 6e), including four units previously defined qualitatively by Sloss (Sauk, Tippecanoe, Zuni/Cretaceous, Tejas/Cenozoic), two units previously defined by Peters (Triassic and Jurassic, which together comprise part of Sloss’ Absaroka), and three new sequences (Kaskaskia 1, Kaskaskia 2/Carboniferous, Permian, which together comprise Sloss’ Kaskaskia and part of the Absaroka). With the exception of Kaskaskia 1 and 2, each of these cratonic sequences is associated with an increase in macrostratigraphic package initiation and/or truncation rate (asterisks in Figs. 4d and 6d). Our proposed separation of Kaskaskia 1 and 2 is based on two criteria: (1) the observation of a strong  $\sim 56 \text{ Myr}$  oscillation, extracted via singular spectrum analysis, which defines Kaskaskia 1 (Figs. 4b and 6b) and (2) the occurrence of a substantial change in the nature of sedimentation (from siliciclastic-dominated to carbonate-dominated) between Kaskaskia 1 and 2, which coincides with the Devonian/Carboniferous boundary (Peters, 2008).

Cycles in sedimentation of similar duration have also been identified in the European stratigraphic record spanning the upper Norian to middle Eocene (Smith and McGowan, 2005), supporting the hypothesis that the  $\sim 56 \text{ Myr}$  oscillation in sedimentation may be global, and at least partially influenced by eustatic sea-level change. Additional evidence for a eustatic origin of sedimentation cycles comes from a complimentary analysis of the coverage area of marine strata in North America ( $A_{\text{mar}}$ ), which exhibits a  $\sim 55 \text{ Myr}$  oscillation (Fig. 5).

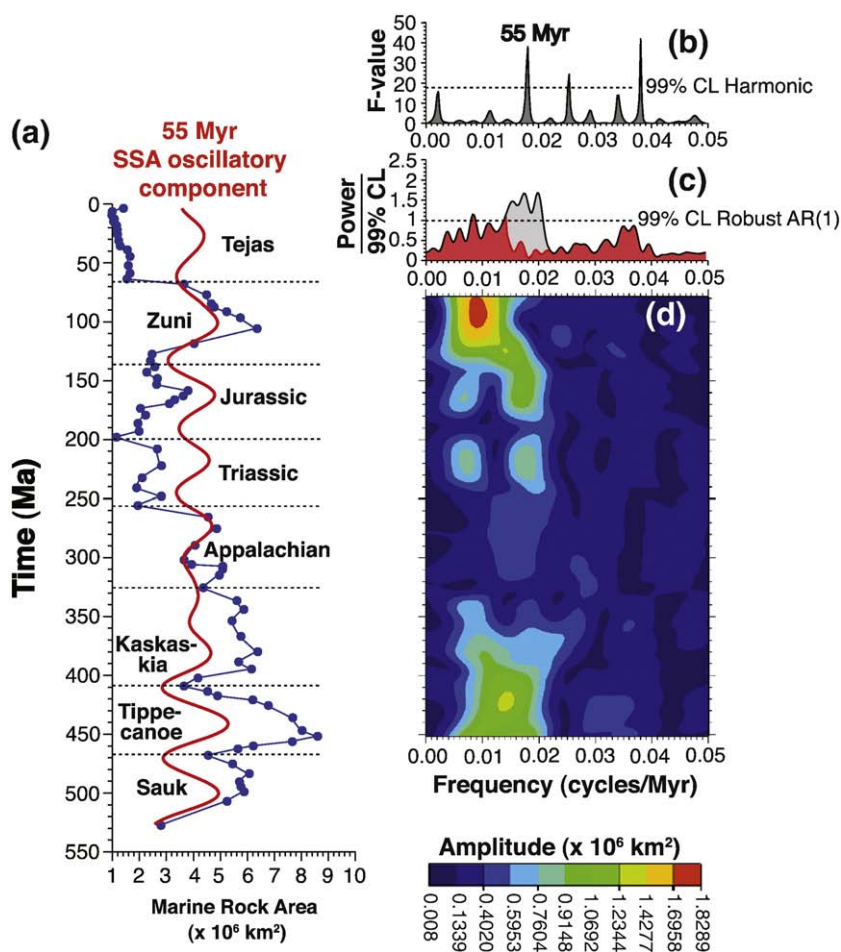


**Fig. 5.** Cyclic variation in North American marine sedimentation. a, Area of preserved marine strata ( $A_{\text{mar}}$ ) in North America during the Phanerozoic (blue), with North American sequences (Peters, 2008; Sloss, 1963) and a 55 Myr oscillatory component extracted using SSA (red). b, MTM harmonic F-test spectrum for  $A_{\text{mar}}$ , calculated using three  $2\pi$  prolate tapers (Thomson, 1982). Dashed line indicates the 99% the confidence levels for F-values. c, MTM power spectrum for  $A_{\text{mar}}$ , calculated using adaptive weighting and three  $2\pi$  prolate tapers (Thomson, 1982). Total power has been divided by the 99% confidence level for a robust AR(1) red noise model (Mann and Lees, 1996). Grey area indicates power attributable to the 55 Myr phase-coherent sinusoid identified in part b, following spectral reshaping (Thomson, 1982). d, EHA of  $A_{\text{mar}}$ , using three  $2\pi$  prolate tapers and a 150 Myr moving window. A linear trend has been removed from each 150 Myr data window prior to harmonic analysis.

The identification of a significant, long-period rhythm in the extent of sedimentation on the North American continent is a novel result that demands the presence of a large-scale oscillatory forcing mechanism. DeCelles et al. (2009) recently proposed such a mechanism for generating long-term cycles in orogenic activity, and this hypothesis may help to explain the origin of cratonic sequences (Sloss, 1963) and the quantitative periodic signal documented here. The orogenic oscillator hypothesis (DeCelles et al., 2009) invokes upper plate processes operating at ocean–continent convergent margins, and a  $\sim 50$  Myr cycle in magmatic activity in the Sierra Nevada batholith is comparable to the  $\sim 56$  Myr cycle we observe in the extent of sedimentation. A link between orogenesis and sedimentation is expected because crustal uplift and subsidence are one determinant of the extent to which sediments are delivered to and accumulate on continental crust. Importantly, the history of ocean–continent convergence in North America is dominated by east coast orogenesis during the Palaeozoic, and west coast orogenesis during the Mesozoic and Cenozoic, potentially yielding two geographically distinct oscillators. Diminishment of the  $\sim 56$  Myr  $A_{\text{sed}}$  cycle during the Carboniferous could be the consequence of interference between an eastern (Acadian orogeny) and western (Antler orogeny) oscillatory forcing during this time.

Quasi-periodic mantle plume formation (Mjeldre and Faleide, 2009; Prokoph et al., 2004; Ribe et al., 2007), hypothesized to occur

based on experimental laboratory simulations (Schaeffer and Manga, 2001), represents an alternative mechanism for generating the observed  $\sim 56$  Myr beat in North American sedimentation. Mantle plume formation is expected to influence sedimentation on the continents by forcing eustatic sea-level changes and by affecting the average freeboard of the continents. The link between mantle plume formation and continent-scale stratigraphic patterns would be further accentuated by climate interactions (Miller et al., 2005), whereby global warming due to increased rates of mantle degassing results in higher sea-levels (e.g., via ice sheet melting and thermal expansion) and wider areas of marine sedimentation on the continents.

A longer-term Phanerozoic mode in sedimentation (Figs. 4a and 6a), linked to the well-known “M-curve” or Wilson cycle of supercontinent coalescence and breakup (Heller and Angevine, 1985; Peters, 2008), is also identified quantitatively in these data. This important Phanerozoic mode defines two mega-sequences, one that spans the Palaeozoic and another that spans the Mesozoic/Cenozoic. Our analysis indicates that this signal is indistinguishable from a stochastic autoregressive process at the 99% confidence level (Figs. 3c and 5c), although the length of the data series limits our ability to detect oscillatory modes on such timescales. This result implies that the physical mechanism responsible for the supercontinent cycle and mega-sequence formation is potentially comprised of two components: (1) a Gaussian white-noise source (for example,

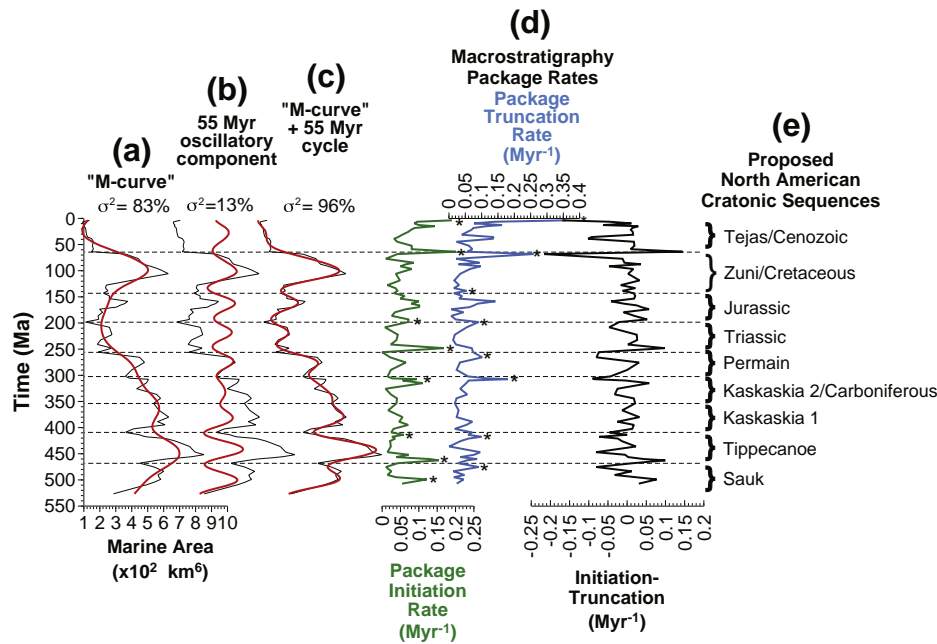


**Fig. 6.** Singular spectrum analysis (SSA) results for the  $A_{\text{mar}}$  data series, as compared to macrostratigraphy package rates. The  $A_{\text{mar}}$  data series is shown as a thin black line, and the SSA reconstructions are shown in red. SSA utilizes an embedding dimension of 80 with the Vautard and Ghil covariance estimator (Ghil et al., 2002), and extracts four dominant reconstructed components (RCs). a, RC 1 and RC 2 (combined), which comprise the long term Phanerozoic “M-curve”. b, RC 3 and RC 4 (combined) constitute an oscillatory pair with variance concentrated at a frequency of  $\sim 1/55 \text{ Myr}^{-1}$ . c, Total SSA reconstruction, which incorporates RC 1, RC 2, RC 3 and RC 4, and accounts for 96% of the variance in  $A_{\text{mar}}$ . d, Package initiation rate (green), package truncation rate (blue), and initiation rate–truncation rate (black), determined by macrostratigraphic analysis. Initiation and truncation rates are calculated according to the estimated per-package per million-year rate adapted from Foote (2000). e, Designation of major North American cratonic sequences based on macro-cyclostratigraphic analysis. (For interpretation of the references to color in this figure legend, the reader is referred to the web version of this article.)

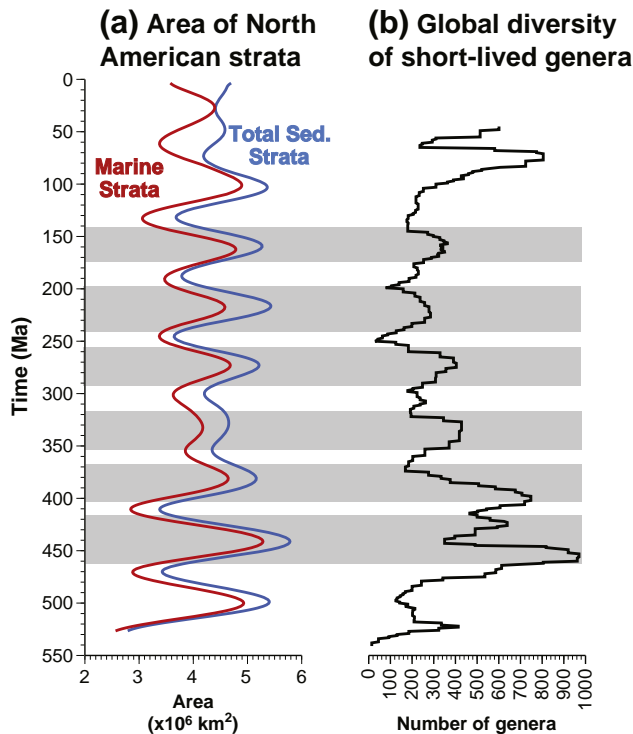


**Fig. 7.** Comparison of the  $\sim 56 \text{ Myr}$  oscillatory signal extracted from the North American stratigraphic record, and global fossil biodiversity data. (a) The  $\sim 56 \text{ Myr}$  SSA oscillatory component derived from  $A_{\text{mar}}$  (red line) and the  $\sim 56 \text{ Myr}$  SSA oscillatory component derived from  $A_{\text{sed}}$  (blue line). (b) The diversity of short-lived genera during the Phanerozoic (Rhode and Muller, 2005). (For interpretation of the references to color in this figure legend, the reader is referred to the web version of this article.)

due to changes in heat production within the core), and (2) an Earth system component/interaction with the appropriate memory time-scale (response time) to integrate the white-noise, producing the observed “M-curve”.

In addition to yielding insight into the characteristics of North American stratigraphic sequences and the nature of cyclic controls on sedimentation on the continents, our results have important implications for the Phanerozoic record of biologic diversity. Previous work has identified a pronounced  $62 \text{ Myr} \pm 3 \text{ Myr}$  cycle in the number of marine genera (Rhode and Muller, 2005), which is statistically similar to the  $56 \text{ Myr} \pm 3 \text{ Myr}$   $A_{\text{sed}}$  cycle that we observe in North American sedimentation (Fig. 7). Thus, cyclical variation in global diversity is likely to be either the consequence of a fossil preservation bias (Peters and Foote, 2001; Smith, 2001; Smith, 2007; Smith and McGowan, 2007), or, more likely, related to global environmental changes that are directly (Hallam, 1989; Johnson, 1974; Newell, 1952; Sepkoski, 1976; Simberloff, 1974) or indirectly linked to the expansions and contractions of epicontinental seas (Hallam and Wignall, 1999; Peters, 2008). The strong covariation of sedimentologic and faunal records during the Phanerozoic is further underscored by the coincidence of many North American cratonic sequences with geologic system boundaries, most of which were originally defined on the basis of biological turnover, but that also occur in phase with a prominent, but as-yet poorly understood, large-scale rhythm in our planet.

## 5. Conclusions

In this study, we apply emerging macrostratigraphic and cyclostratigraphic methodologies to quantitatively evaluate temporal modes (“orders”) of stratigraphic variability across the North American continent during the Phanerozoic. Macrostratigraphic

analysis provides an estimate of the total coverage area of sedimentary strata (surface and subsurface), as well as quantitative measures of the underlying processes that generate the observed stratigraphy (rates of initiation and termination of sedimentary packages). Quantitative cyclostratigraphic methods provide the opportunity to objectively identify stratigraphic “orders” in the macrostratigraphic data, and permit the deconvolution of deterministic sinusoidal modes from stochastic variability.

Analysis of the total coverage area of sedimentary strata (terrestrial + marine) identifies two prominent modes: (1) a strongly sinusoidal mode with a periodicity of 56 Myr  $\pm$  3 Myr, and (2) a longer-term Phanerozoic mode (the “M-curve” or Wilson cycle), which is indistinguishable from a stochastic autoregressive process. Similar temporal modes are obtained from an analysis of the coverage area of marine sedimentary strata during the Phanerozoic. Based on these results we propose a quantitative redefinition of the North American cratonic sequences, with nine distinct units (Sauk, Tippecanoe, Kaskaskia 1, Kaskaskia 2/Carboniferous, Permian, Triassic, Jurassic, Zuni/Cretaceous, and Tejas/Cenozoic) and two mega-sequences (Palaeozoic and Mesozoic/Cenozoic).

The ~56 Myr beat in North American sedimentation is statistically similar to a known rhythm in number of marine animal genera in the global fossil record, indicating either a fossil preservation bias that impacts observed biodiversity, or an intimate linkage between sea-level and environmental conditions that influence biodiversity. The source of this ~56 Myr rhythm remains uncertain, but it must ultimately derive from a tectonic- and/or mantle-scale cyclic process. Importantly, these results suggest a unified oscillatory mechanism that links North American cratonic sequences, geodynamics, and changes in observed biologic diversity, throughout the Phanerozoic.

## Acknowledgments

This research was partially funded by National Science Foundation grants to SEP (NSF EAR 0819931) and SRM (NSF EAR 1003603). We thank Nereo Preto, Graham Weedon, and Peggy Delaney for providing very helpful reviews and editorial comments on the manuscript.

## Appendix A. Supplementary data

Supplementary data to this article can be found online at doi:[10.1016/j.epsl.2010.12.044](https://doi.org/10.1016/j.epsl.2010.12.044).

The Supplementary data are available in two separate EXCEL files. The first is designated as “Electronic Appendix 1” and contains Macrostratigraphic data for total sedimentary strata. The second is designated as “Electronic Appendix 2” and contains Macrostratigraphic data for marine sedimentary strata.

## References

- Childs, O.E., 1985. Correlation of stratigraphic units of North America; COSUNA. AAPG Bull. 69, 173–180.
- Clark, P.U., Alley, R.B., Pollard, D., 1999. Northern Hemisphere Ice-sheet influences on global climate change. *Science* 286, 1104–1111.
- DeCelles, P.G., Ducea, M.N., Kapp, P., Zandt, G., 2009. Cyclicity in Cordilleran orogenic systems. *Nat. Geosci.* 2, 251–257.
- Douglas, R.J.W., 1970. Geology and economic minerals of Canada. Economic Geology Report No. 1. Geological Survey of Canada, Ottawa.
- Foote, M., 2000. Origination and extinction components of taxonomic diversity: general problems. *Paleobiology* 4, 74–102.
- Ghil, M., Allen, M.R., Dettinger, M.D., Ide, K., Kondrashov, D., Mann, M.E., Robertson, A.W., Saunders, A., Tian, Y., Varadi, F., Yiou, P., 2002. Advanced spectral methods for climatic time series. *Rev. Geophys.* 40 1–1–1–41.
- Hallam, A., 1989. The case for sea-level change as a dominant casual factor in mass extinction. *Proc. R. Soc. Lond. B* 325, 437–455.
- Hallam, A., Wignall, P.B., 1999. Mass extinction and sea-level changes. *Earth Sci. Rev.* 48, 217–250.
- Hannisdal, B., Peters, S.E., 2010. On the relationship between macrostratigraphy and geological processes: quantitative information capture and sampling robustness. *J. Geol.* 118 (2), 111–130.
- Haq, B.U., Hardenbol, J., Vail, P., 1987. Chronology of fluctuating sea levels since the Triassic. *Science* 235, 1156–1167.
- Hays, J.D., Imbrie, J., Shackleton, N.J., 1976. Variations in the Earth's orbit: pacemaker of the ice ages. *Science* 194, 1121–1132.
- Heller, P.L., Angevine, C.L., 1985. Sea-level cycles during the growth of Atlantic-type oceans. *Earth Planet. Sci. Lett.* 75, 417–426.
- Johnson, J.G., 1974. Extinction of perched faunas. *Geology* 2, 479–482.
- Kominz, M.A., 1995. Thermally subsiding basins and the effect of sediments with application to the Cambro-Ordovician Great Basin sequence, western U.S. *Basin Res.* 7, 221–233.
- Lisiecki, L.E., 2010. Links between eccentricity forcing and the 100,000-year glacial cycle. *Nat. Geosci.* 3, 349–352.
- Mann, M.E., Lees, J.M., 1996. Robust estimation of background noise and signal detection in climatic time series. *Climate Change* 33, 409–445.
- Meyers, S., Sageman, B., Hinnov, L., 2001. Integrated quantitative stratigraphy of The Cenomanian–Turonian bridge creek limestone member using evolutive harmonic analysis and stratigraphic modeling. *J. Sed. Res.* 71, 627–643.
- Meyers, S.R., Sageman, B.B., Pagani, M., 2008. Resolving Milankovitch: consideration of signal and noise. *Am. J. Sci.* 308, 770–786.
- Miall, A.D., 1997. *The Geology of Stratigraphic Sequences*. Springer-Verlag, Berlin. 433 pp.
- Miller, K.G., Kominz, M.A., Browning, J.V., Wright, J.D., Mountain, G.S., Katz, M.E., Sugarman, P.J., Cramer, B.S., Christie-Blick, N., Pekar, S.F., 2005. The Phanerozoic Record of Global Sea-Level Change. *Science* 310, 1293–1298.
- Mjelde, R., Faleide, J.J., 2009. Variation of Icelandic and Hawaiian magmatism: evidence for co-pulsation of mantle plumes? *Mar. Geophys. Res.* 30, 61–72. doi:[10.1007/s11001-009-9066-0](https://doi.org/10.1007/s11001-009-9066-0).
- Newell, N.D., 1952. Periodicity of invertebrate evolution. *J. Paleontol.* 26, 371–385.
- Peters, S.E., 2006. Macrostratigraphy of North America. *J. Geol.* 114, 391–412.
- Peters, S.E., 2008. Macrostratigraphy and its promise for paleobiology. *Paleontol. Soc. Pap.* 14, 205–231.
- Peters, S.E., Foote, M., 2001. Biodiversity in the Phanerozoic: a reinterpretation. *Paleobiology* 27, 583–601.
- Peters, S.E., Heim, N.A., 2010. The geological completeness of paleontological sampling in North America. *Paleobiology* 36, 61–79.
- Prokoph, A., Ernst, R.E., Buchan, K.L., 2004. Time-series analysis of large igneous provinces: 3500 Ma to present. *J. Geol.* 112, 1–22.
- R development core team, 2006. R: a language and environment for statistical computing. R Foundation for Statistical Computing, Vienna, Austria. <http://www.R-project.org> 2006 URL.
- Rhode, R.A., Muller, R.A., 2005. Cycles in fossil diversity. *Nature* 434, 208–210.
- Ribe, N., Davaille, A., Christensen, U., 2007. Fluid dynamics of mantle plumes. In: Ritter, J., Christensen, U. (Eds.), *Mantle Plumes: A Multidisciplinary Approach*. Springer, Berlin. pp. 1–48.
- Salvador, A., 1985. Chronostratigraphic and geochronometric scales in COSUNA stratigraphic correlation charts of the United States. AAPG Bull. 69, 181–189.
- Schaeffer, N., Manga, M., 2001. Interaction of rising and sinking mantle plumes. *Geophys. Res. Lett.* 28, 455–458.
- Sepkoski Jr., J.J., 1976. Species diversity in the Phanerozoic: species-area effects. *Paleobiology* 2, 298–303.
- Simberloff, D.S., 1974. Permo-Triassic extinctions: effects of area on biotic equilibrium. *J. Geol.* 82, 267–274.
- Sloss, L.L., 1963. Sequences in the cratonic interior of North America. *Geologic Soc. Am. Bull.* 74, 93–113.
- Smith, A.B., 2001. Large-scale heterogeneity of the fossil record: implications for Phanerozoic biodiversity studies. *Philos. Trans R. Soc. Lond. B* 356, 351–367.
- Smith, A.B., 2007. Marine diversity through the Phanerozoic: problems and prospects. *J. Geol. Soc.* 164, 731–745.
- Smith, A.B., McGowan, A.J., 2005. Cyclicity in the fossil record mirrors rock outcrop area. *Biol. Lett.* 1, 443–445.
- Smith, A.B., McGowan, A.J., 2007. The shape of the Phanerozoic diversity curve. How much can be predicted from the sedimentary rock record of Western Europe? *Paleontology* 50, 1–10.
- Thomson, D.J., 1982. Spectrum estimation and harmonic analysis. *IEEE Proc.* 70, 1055–1096.
- Vail, P.R., Mitchum Jr., R.M., Todd, R.G., Widmier, J.M., Thompson III, S., Sangree, J.B., Bub, J.N., Hatfield, W.G., 1977. Seismic stratigraphy and global changes of sea level. In: Payton, C.E. (Ed.), *Seismic Stratigraphy—Applications to Hydrocarbon Exploration*: American Association Petroleum Geologists Memoir, 26, pp. 49–212.
- Zachos, J., Pagani, M., Sloan, L., Thomas, E., Billups, K., 2001. Trends, rhythms, and aberrations in global climate 65 Ma to present. *Science* 292, 686–693.